

The dark timbre of gravitational waves

Juan Urrutia^{1,2,*} and Ville Vaskonen^{1,3,4,†}

¹*Keemilise ja Bioloogilise Füüsika Instituut, Rävåla pst. 10, 10143 Tallinn, Estonia*

²*Department of Cybernetics, Tallinn University of Technology, Akadeemia tee 21, 12618 Tallinn, Estonia*

³*Dipartimento di Fisica e Astronomia, Università degli Studi di Padova, Via Marzolo 8, 35131 Padova, Italy*

⁴*Istituto Nazionale di Fisica Nucleare, Sezione di Padova, Via Marzolo 8, 35131 Padova, Italy*

Gravitational wave timbre, the relative amplitude and phase of the different harmonics, can change due to interactions with low-mass halos. We focus on binaries in the LISA range and find that the integrated lens effect of cold dark matter structures can be used to probe the existence of $M_v \lesssim 10 M_\odot$ halos if a single binary with eccentricity $e = 0.3 - 0.6$ is detected with a signal-to-noise ratio $100 - 10^4$.

Introduction – Gravitational waves (GWs) are often associated with sound because they are characterized by waveforms and in general, there is a poorer angular resolution than with electromagnetic signals. Like with sound, for GWs there is also the notion of timbre since eccentric binaries emit GWs in different harmonics simultaneously. The relative powers of the harmonics are determined by the binary eccentricity and the harmonic numbers [1].

GWs are sensitive to wave optics interactions with small halos which can leave detectable imprints in the waveform [2–9] or a phase difference with respect to an electromagnetic counterpart [10–13]. Both methods rely on frequency-dependent effects for detectability.

In this work, we propose a novel probe of the wave optics effects: measurements of the timbre of the GW signal from an eccentric binary. Furthermore, we considered not only the effect of a single encounter but the integrated effect of light halos which the GW signal is expected to encounter. We study if the measurements of the timbre can be used to probe the low mass end of the dark matter (DM) halo mass function (HMF) where deviations from the cold dark matter (CDM) predictions may appear. For example, the small-scale structures are suppressed in models of warm or ultralight DM models [14–16].

We focus on signals whose frequency does not change significantly. In the LISA sensitivity range, such signals can originate e.g. from intermediate-mass black holes or extreme mass ratio binaries [17–22]. We compute the integrated effect of the DM halo population and show that very light halos, which are integrated out in weak lensing studies as a constant density field [23], induce changes in the amplitude and phases of the different harmonics of a mHz GW signal, effectively changing the timbre by the imprints of these light DM structures. The effect is detectable with LISA in the first harmonics if the binary has a signal-to-noise between $100 - 10^4$ and has eccentricity $e = 0.3 - 0.6$. We find that the effect mainly comes from halos of $\mathcal{O}(10 M_\odot)$. Such light halos are a prediction of CDM but so far have eluded observations [24]. Therefore, its detection would provide a probe of the low mass tail of the HFM and severely constraint deviations

from CDM at small scales.

Lensing by a single halo – Consider a binary whose orbital frequency remains almost constant during the observation. We denote the angular diameter distance of the binary by $D_s = d_c(z_s)/(1+z_s)$, where z_s is the corresponding redshift and d_c is the comoving distance, and assume that the GW signal emitted by the binary interacts with a halo at angular diameter distance D_l . In the frequency domain, the lensed waveform is $\tilde{\phi}_L(f) = F(f)\tilde{\phi}(f)$, where $\tilde{\phi}(f)$ denotes the unperturbed GW signal. The amplification factor $F(f)$ in the thin-lens approximation is given by [25]

$$F(f) = \frac{w(f)}{2i\pi} \int d^2\mathbf{x} e^{iw(f)T(\mathbf{x},\mathbf{y})}, \quad (1)$$

which is an integral over the lens plane of all the paths that the GW can take through it and the prefactor ensures that in the absence of the lens $F(f) = 1$. We define a characteristic length scale ξ_0 and dimensionful vectors that denote the position of the source ($\boldsymbol{\eta}$) in the source plane and the position at which the GW crosses the lens plane ($\boldsymbol{\chi}$). The dimensionless vectors \mathbf{x} and \mathbf{y} are defined as $\mathbf{x} \equiv \boldsymbol{\xi}/\xi_0$ and $\mathbf{y} \equiv D_l\boldsymbol{\eta}/(D_s\xi_0)$. The dimensionless frequency w and the dimensionless time delay function T then become

$$w(f) \equiv \frac{(1+z_l)D_s}{D_l D_{ls}} \xi_0^2 2\pi f, \quad (2)$$

$$T(\mathbf{x}, \mathbf{y}) \equiv \frac{1}{2} |\mathbf{x} - \mathbf{y}|^2 - \psi(\mathbf{x}) - \phi(\mathbf{y}), \quad (3)$$

where $D_{ls} = D_s - (1+z_l)/(1+z_s)D_l$ and $\phi(\mathbf{y})$ is defined such that $\min_{\mathbf{x}} T(\mathbf{x}, \mathbf{y}) = 0$.

We approximate the halos by the NFW profile $\rho(r) = r_s^3 \rho_s / [r(r_s + r)^2]$, which corresponds to the lens potential (see e.g. [3])

$$\psi(x) = \kappa \left[\ln^2\left(\frac{x}{2b}\right) - \operatorname{artanh}^2 \sqrt{1 - \frac{x^2}{b^2}} \right], \quad (4)$$

where $x = |\mathbf{x}|$ and $\kappa \equiv 2\pi\rho_s r_s^3 / M_v$ and $b \equiv r_s / \xi_0$ are dimensionless parameters. The distances are scaled by $\xi_0 = R_E(M_v)$, where R_E denotes the point mass Einstein

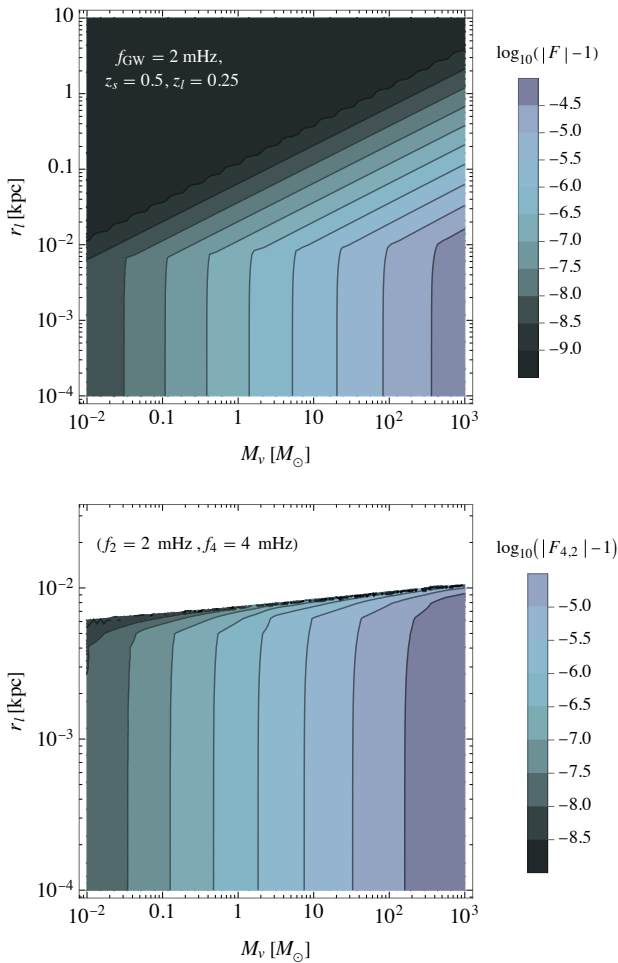


FIG. 1. *Upper panel:* The absolute value of the lensing amplification as a function of the halo mass and the projected distance of the source in the lens plane, for a source with $f_{\text{GW}} = 2$ mHz, $z_s = 0.5$ and $z_l = 0.25$. *Lower panel:* The magnitude of the relative amplification factor (7) for the same GW and source-lens configuration as in the upper panel.

radius, so the dimensionless frequency simplifies to $w = 8\pi(1+z_l)M_v f$. The NFW profile is parameterized by the scale radius r_s and the corresponding density ρ_s , which are both functions of the halo virial mass M_v . For halos as light as the ones we will consider interactions with stars can affect the profile. However, the survival rate is expected to be high [26–32] so we can safely use the NFW profile.

In the geometric limit, the GW follows a single classical trajectory, the minimal time path, around the NFW halo. The interaction lacks interference patterns and induces a frequency-independent amplification [2],

$$|F| = (\det[\partial_a \partial_b T(\mathbf{x}_j, y)])^{-2}, \quad (5)$$

where $y = |\mathbf{y}|$ and \mathbf{x}_j corresponds to the classical path. However, in the wave optics regime, the amplification becomes frequency dependent, and numerical computation

of Eq. (1) is necessary.¹

In the upper panel of Fig. 1, we show the amplification $|F|$ for different halo masses and distances in the lens plane. We have fixed the signal frequency to $f_{\text{GW}} = 2$ mHz, the source redshift to $z_s = 0.5$, and the lens is positioned at half the redshift. For a fixed halo mass in the wave optics regime, the interaction is independent of the projected position $r_l \equiv \xi_0 y$ of the source in the lens plane. In the geometric optics regime, the amplification effect rapidly decreases with r_l , roughly as $|F| - 1 \propto r_l^{-4}$ but increases with the lens mass,² roughly as $|F| - 1 \propto M_v^{7/6}$. The dividing distance between the wave optics and geometric optics regimes, on the other hand, increases very slowly with M_v remaining slightly below $r_l \approx 10$ pc in the shown mass range.

Whereas a circular binary emits GWs only at twice its orbital frequency, an eccentric binary emits at all integer multiples of it [1],

$$f_n = n f_{\text{orb}}. \quad (6)$$

The different harmonics get amplified by different amounts as the lensing effect is frequency-dependent. This is the dark timbre effect. In the lower panel of Fig. 1, we show the magnitude of the ratio of amplification factors that characterize the shift in the timbre,

$$F_{i,j} \equiv \frac{|F(f_i)|}{|F(f_j)|} e^{i\Delta\phi_{i,j}}, \quad \Delta\phi_{i,j} \equiv \phi_i - \phi_j, \quad (7)$$

between the second and the fourth harmonic of an eccentric binary with orbital frequency $f_{\text{orb}} = 1$ mHz. As expected, there is no difference in the geometric optics regime’s amplification factor for high-impact parameters. Only the halos in the wave optics regime, $r_l < 10$ pc, modify the timbre of the signal. The phase difference is similar in magnitude to the amplification factor ratio.

Total lens effect – The effect of a single lens is characterized by the lens redshift z_l , the projected distance of the source in the lens plane r_l and the halo mass M_v . We estimate the modification of the timbre caused by all of the halos the signal encounters in the wave optics regime on its way from the source to the detector by generating configurations of the heaviest lenses and estimating the expected effect from the light halos.

We consider only halos inside the wave optics regime, $r_l < r_{\text{max}}(z_l, M_v)$, since those are the only ones causing a frequency dependent effect. The total number of halos within that radius is

$$N = \int dM_v \int_0^{z_s} dz_l \int_0^{r_{\text{max}}} dr_l \frac{2\pi r_l}{H(z_l)(1+z_l)} \frac{dn(z_l)}{dM_v}, \quad (8)$$

¹ We do it by computing the method introduced in [33].

² Linear scaling $|F| - 1 \propto M_v$ at a fixed frequency is expected if κ and b didn’t change with M_v . We find a slightly stronger scaling mainly because the compactness of the halos mildly decreases with decreasing M_v .

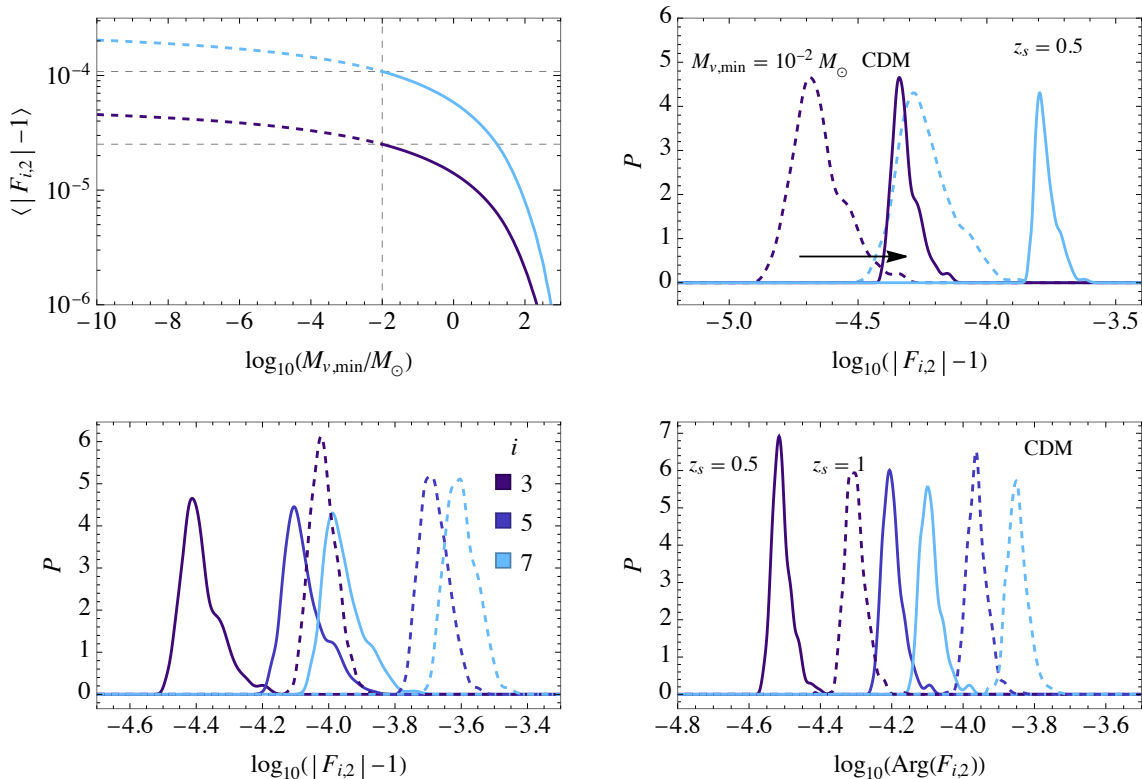


FIG. 2. *Upper panels:* The left plot shows the expected value for $|F_{i,2}| - 1$ for the third and seventh harmonic when integrating the halos from $M_{v,\min}$. The right plot shows how the distributions from the heavy halos, $M_v > 10^{-2}M_\odot$, (dashed curves) change when adding the contribution from the light ones. *Lower panels:* The probability distributions of $|F_{i,2}| - 1$ and $\text{Arg}(F_{i,2})$ for $i = 3, 5, 7$ and a source with $f_2 = 2$ mHz at $z_s = 0.5$ (solid) and $z_s = 1$ (dashed).

where $dn(z_l)/dM_v$ is the HMF which we compute using the extended Press-Schechter formalism [34, 35] with the CDM power spectrum [36]. From Eq. (8), we can identify the probability densities of the lens parameters:

$$P(z_l, M_v) = \frac{\pi r_{\max}^2}{NH(z_l)(1+z_l)} \frac{dn(z_l)}{dM_v}, \quad (9)$$

$$P(r_l|z_l, M_v) = \theta(r_l - r_{\max}) \frac{2r_l}{r_{\max}^2}.$$

We generate realizations of the lenses with mass $M_v > 0.01M_\odot$ that the signal encounters by sampling the probability distributions (9) and approximate their total effect by taking a product of the amplifications caused by each of the lenses:

$$F_H(f) = \prod_{j=1}^{N_h} F(f|M_{v,j}, z_{l,j}, r_{l,j}) \quad (10)$$

$$\approx 1 + \sum_{j=1}^{N_h} [F(f|M_{v,j}, z_{l,j}, r_{l,j}) - 1].$$

Here N_h is sampled from a Poisson distribution with mean N in the mass range $M_v > 0.01M_\odot$ and the approximation holds because $F(f|M_{v,j}, z_{l,j}, r_{l,j}) \approx 1$. We

generate 10^3 realizations to estimate the distribution of $F_H(f)$.

For light halos with $M_v < 0.01M_\odot$, the Poisson fluctuations are negligible because their number inside the wave optics regime is very large. Therefore, the effect they cause does not change significantly between different paths and the distribution of the total lensing factor

$$F_{\text{tot}}(f) = F_H(f)F_L(f) \approx F_H(f) + F_L(f) - 1 \quad (11)$$

can then be estimated by convoluting the distribution of F_H with $\delta(F - F_L + 1)$, where

$$F_L(f) = \sum_j [1 + \langle F(f) - 1 \rangle_j N_{h,j} (1 - e^{-N_{h,j}})] \quad (12)$$

is the expected effect from the light halos. The sum in (12) is over mass bins, $\langle F(f) - 1 \rangle_j$ is the expected deviation of the lensing factor from unity for halos in the mass bin j and $N_{h,j}$ is the number of halos in the wave optics regime in that bin. This results in a translation of the distribution from heavy halos by adding the integrated effect of the light ones.

In the upper panels of Fig. 2 we show what is the effect of adding the lightest halos. On the left panel, we can

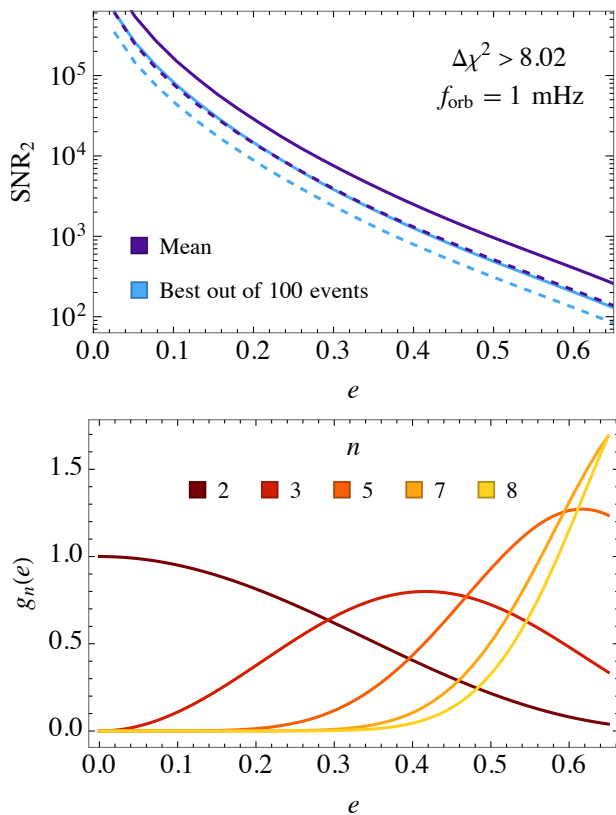


FIG. 3. *Upper panel:* The SNR of the second harmonic (SNR_2) necessary for detection of the shifted timbre as a function of the eccentricity of a binary orbiting at 1 mHz. The dark and light curves correspond, respectively, to a source at $z_s = 1$ and at $z_s = 0.5$. The solid lines correspond to the mean values of the amplifications and the dashed ones to the best 1%. *Lower panel:* The relative powers $g_n(e)$ of some of the lowest harmonics.

see how halos heavier than $100 M_\odot$ are not contributing significantly. The reason for that is that they are too rare to fill the wave optics lensing tube. The main effect comes from halos between $10^{-2} - 10 M_\odot$ being $10 M_\odot$ the ones that give the biggest contribution. Beyond $10^{-2} M_\odot$ the effect increases very slowly and we have explicitly checked that it converges. Halos lighter than $10^{-2} M_\odot$ change the total lensing effect by an $\mathcal{O}(1)$ factor. On the right panel, we can see how the distributions are shifted by adding the contribution from the lightest halos.

In the lower panels of Fig. 2 we show the probability distribution of the modulus and the argument of the amplification ratio between the second and the third, the fifth and the seventh harmonic for the same benchmark case as in Fig. 1, for $z_s = 0.5$ (solid lines) and $z_s = 1$ (dashed lines). On the left panel, we see that the differences are of order 10^{-4} for $z_s = 0.5$ and up to 3×10^{-4} for $z_s = 1$. We can see that the distribution of the phase difference scales as expected concerning the amplifications, goes up to 3×10^{-5} or 6×10^{-5} for $z_s = 0.5$ and $z_s = 1$

respectively.

Previous GW microlensing studies have focused on searching for halos with $M_v \gtrsim 10^6 M_\odot$, which causes a larger effect. However, for realistic profiles like either Einasto [37] or NFW, the effect in the geometric limit is just a constant amplification [3] that is degenerate with the rest of the parameters. The lensing tube where wave optics effects are relevant is fixed by the frequency of the GW and the mass of the halo. For the LISA frequencies and halos with $M_v \gtrsim 10^6 M_\odot$ the expected number of halos in the wave optics tube is very small and, consequently, it is not expected that LISA would see any such lensed events [3]. In this study, we instead consider much lighter halos $M_v \lesssim 10 M_\odot$ which are expected, assuming the CDM model, to induce wave optics effects in all of the GW events that LISA will see. The next section discusses the precision necessary to test and detect this effect.

Detectability and prospects – To detect this effect, we require that the signal with the shifted timbre can not fit well with a template using the standard timbre. In general, the wellness of a template fit is given by [38]

$$\Delta\chi^2 = 4 \min_{\vec{\theta}} \int df \frac{|\tilde{h}(f) - \tilde{h}_T(f, \vec{\theta})|^2}{S(f)}, \quad (13)$$

where $\tilde{h}(f)$ refers to the GW signal and $\tilde{h}_T(f, \vec{\theta})$ the template parameterized by $\vec{\theta}$. For a binary that evolves very slowly, the waveform is approximately a sum of delta functions and Eq. (13) simplifies to

$$\begin{aligned} \Delta\chi^2 &= 4 \min_{\lambda, \phi, e'} \sum_{n=1}^{\infty} \frac{A^2 |F(f_n) \sqrt{g_n(e)} - \lambda e^{i\phi} \sqrt{g_n(e')}|^2}{S(f_n)} \\ &= \frac{\text{SNR}_2^2}{g_2(e)} \min_{\lambda, \phi, e'} \sum_{n=1}^{\infty} \frac{S(f_2)}{S(f_n)} \left| F_{n,2} \sqrt{g_n(e)} - \lambda e^{i\phi} \sqrt{g_n(e')} \right|^2, \end{aligned} \quad (14)$$

where A characterizes the amplitude of the signal and SNR_2 is the signal-to-noise ratio of the second harmonic. The template is parameterized by an amplitude $\lambda \approx 1$, an eccentricity $e' \approx e$, and a phase $\phi \approx 0$. The function $g_n(e)$ is the relative power radiated in the n th harmonic by a binary with eccentricity e [1]. We show $g_n(e)$ for some of the lowest harmonics in the lower panel of Fig. 3.

For the spectral sensitivity $S(f)$ we use the proposed spectral sensitivity for LISA [39, 40] including the galactic and extragalactic foregrounds [41]. We considered sources at $z_s = 0.5$ and at $z_s = 1$ with $f_2 = 2$ mHz. To assess the detectability of the shifted timbre effect, we consider only the harmonics $n = 2 - 7$ which dominate the signal for $e < 0.6$, as seen in the lower panel of Fig. 3. As benchmarks, we consider 1) the mean values for $F_{i,2}$ and 2) the best out of 100 events. We determine how large SNR_2 needs to be for a given e so that the shifted timbre is detectable. We use the threshold $\Delta\chi^2 > 8.02$ corresponding to 2σ CL for a template with three parameters. In the upper panel of Fig. 3, we show

that if we consider $z_s = 0.5$ (full lines) then $\text{SNR}_2 \sim 10^4$ is required if $e = 0.3$ but for $e = 0.5$ it is enough to have $\text{SNR}_2 \lesssim 10^3$. The required SNR_2 is about a factor 3 smaller for the best out of 100 events than for the mean. These SNRs seem within the reach of LISA for sufficiently nearby sources.

The precision at which the amplitudes of a harmonic i can be resolved is

$$\frac{\sigma_{A_i}}{A_i} = \frac{1}{\text{SNR}_i}, \quad (15)$$

which is easy to show from Fisher analysis [42]. This implies that a higher SNR_2 is necessary to resolve the relative amplification factors $F_{i,j}$ than to detect the dark timbre. Optimistically, if a population of eccentric binaries is detected with $\text{SNR}_i \sim 10^4$ it would be possible to reconstruct the PDFs of $F_{i,j}$ and probe the HMF down to $M_V \ll 10 M_\odot$. However, already the detection of one sufficiently eccentric binary with $\text{SNR}_2 \gtrsim 10^3$ would tell about the existence of halos with $M_V \lesssim 10 M_\odot$.

Conclusions – We have estimated for the first time the integrated lensing effect of light halos on the mid-frequency (mHz) gravitational wave signals. We have proposed to test these effects using the different harmonics of an eccentric binary. We have shown that the wave optics effects due to the low mass dark matter halos, $M_V \lesssim 10 M_\odot$, induce frequency-dependent changes in the amplitude and phase of the harmonics, the timbre of the signal. This shifted timbre is detectable in the 7 dominant harmonics of the signal for signal-to-noise ratios between $500 - 10^4$ if the binary eccentricity is $e = 0.3 - 0.6$. If such binaries exist, LISA could probe the shifted timbre. This would open a new avenue to test low-mass dark matter halos and thus provide new insights into the nature of dark matter.

Acknowledgments – We thank Luca Marzola and Hardi Veermäe for useful suggestions. This work was supported by the Estonian Research Council grants PRG803, PSG869, RVT3 and RVT7 and the Center of Excellence program TK202. The work of V.V. was partially supported by the European Union’s Horizon Europe research and innovation program under the Marie Skłodowska-Curie grant agreement No. 101065736.

* juan.urrutia@kbfi.ee

† ville.vaskonen@pd.infn.it

- [1] P. C. Peters and J. Mathews, *Phys. Rev.* **131**, 435 (1963).
- [2] R. Takahashi and T. Nakamura, *Astrophys. J.* **595**, 1039 (2003), [arXiv:astro-ph/0305055](https://arxiv.org/abs/astro-ph/0305055).
- [3] M. Fairbairn, J. Urrutia, and V. Vaskonen, *JCAP* **07**, 007 (2023), [arXiv:2210.13436](https://arxiv.org/abs/2210.13436) [astro-ph.CO].
- [4] M. Çalışkan, N. Anil Kumar, L. Ji, J. M. Ezquiaga, R. Cotesta, E. Berti, and M. Kamionkowski, *Phys. Rev. D* **108**, 123543 (2023), [arXiv:2307.06990](https://arxiv.org/abs/2307.06990) [astro-ph.CO].
- [5] S. Savastano, G. Tambalo, H. Villarrubia-Rojo, and M. Zumalacárregui, *Phys. Rev. D* **108**, 103532 (2023), [arXiv:2306.05282](https://arxiv.org/abs/2306.05282) [gr-qc].
- [6] G. Tambalo, M. Zumalacárregui, L. Dai, and M. H.-Y. Cheung, *Phys. Rev. D* **108**, 103529 (2023), [arXiv:2212.11960](https://arxiv.org/abs/2212.11960) [astro-ph.CO].
- [7] H. Ma, Y. Lu, Z. Chen, and Y. Chen, *Mon. Not. Roy. Astron. Soc.* **524**, 2954 (2023), [arXiv:2307.02742](https://arxiv.org/abs/2307.02742) [astro-ph.CO].
- [8] P. Cremonese, J. M. Ezquiaga, and V. Salzano, *Phys. Rev. D* **104**, 023503 (2021), [arXiv:2104.07055](https://arxiv.org/abs/2104.07055) [astro-ph.CO].
- [9] J. Urrutia, V. Vaskonen, and H. Veermäe, *Phys. Rev. D* **108**, 023507 (2023), [arXiv:2303.17601](https://arxiv.org/abs/2303.17601) [astro-ph.CO].
- [10] R. Takahashi, *Astrophys. J.* **835**, 103 (2017), [arXiv:1606.00458](https://arxiv.org/abs/1606.00458) [astro-ph.CO].
- [11] T. Morita and J. Soda, (2019), [arXiv:1911.07435](https://arxiv.org/abs/1911.07435) [gr-qc].
- [12] J. M. Ezquiaga, W. Hu, and M. Lagos, *Phys. Rev. D* **102**, 023531 (2020), [arXiv:2005.10702](https://arxiv.org/abs/2005.10702) [astro-ph.CO].
- [13] T. Suyama, *Astrophys. J.* **896**, 46 (2020), [arXiv:2003.11748](https://arxiv.org/abs/2003.11748) [gr-qc].
- [14] P. Bode, J. P. Ostriker, and N. Turok, *Astrophys. J.* **556**, 93 (2001), [arXiv:astro-ph/0010389](https://arxiv.org/abs/astro-ph/0010389).
- [15] L. Hui, J. P. Ostriker, S. Tremaine, and E. Witten, *Phys. Rev. D* **95**, 043541 (2017), [arXiv:1610.08297](https://arxiv.org/abs/1610.08297) [astro-ph.CO].
- [16] K. K. Rogers and H. V. Peiris, *Phys. Rev. Lett.* **126**, 071302 (2021), [arXiv:2007.12705](https://arxiv.org/abs/2007.12705) [astro-ph.CO].
- [17] L. Barack and C. Cutler, *Phys. Rev. D* **75**, 042003 (2007), [arXiv:gr-qc/0612029](https://arxiv.org/abs/gr-qc/0612029).
- [18] S. Babak, J. Gair, A. Sesana, E. Barausse, C. F. Sopuerta, C. P. L. Berry, E. Berti, P. Amaro-Seoane, A. Petiteau, and A. Klein, *Phys. Rev. D* **95**, 103012 (2017), [arXiv:1703.09722](https://arxiv.org/abs/1703.09722) [gr-qc].
- [19] C. P. L. Berry, S. A. Hughes, C. F. Sopuerta, A. J. K. Chua, A. Heffernan, K. Holley-Bockelmann, D. P. Mihaylov, M. C. Miller, and A. Sesana, (2019), [arXiv:1903.03686](https://arxiv.org/abs/1903.03686) [astro-ph.HE].
- [20] J. R. Gair, S. Babak, A. Sesana, P. Amaro-Seoane, E. Barausse, C. P. L. Berry, E. Berti, and C. Sopuerta, *J. Phys. Conf. Ser.* **840**, 012021 (2017), [arXiv:1704.00009](https://arxiv.org/abs/1704.00009) [astro-ph.GA].
- [21] O. A. Hannuksela, K. W. K. Wong, R. Brito, E. Berti, and T. G. F. Li, *Nature Astron.* **3**, 447 (2019), [arXiv:1804.09659](https://arxiv.org/abs/1804.09659) [astro-ph.HE].
- [22] M. Bonetti and A. Sesana, *Phys. Rev. D* **102**, 103023 (2020), [arXiv:2007.14403](https://arxiv.org/abs/2007.14403) [astro-ph.GA].
- [23] M. Bartelmann and P. Schneider, *Phys. Rept.* **340**, 291 (2001), [arXiv:astro-ph/9912508](https://arxiv.org/abs/astro-ph/9912508).
- [24] J. Zavala and C. S. Frenk, *Galaxies* **7**, 81 (2019), [arXiv:1907.11775](https://arxiv.org/abs/1907.11775) [astro-ph.CO].
- [25] P. Schneider, J. Ehlers, and E. Falco, *Gravitational Lenses*, Astronomy and Astrophysics Library (Springer New York, 2012).
- [26] M. S. Delos, *Phys. Rev. D* **100**, 083529 (2019), [arXiv:1907.13133](https://arxiv.org/abs/1907.13133) [astro-ph.CO].
- [27] E. Hayashi, J. F. Navarro, J. E. Taylor, J. Stadel, and T. R. Quinn, *Astrophys. J.* **584**, 541 (2003), [arXiv:astro-ph/0203004](https://arxiv.org/abs/astro-ph/0203004).
- [28] F. C. van den Bosch, G. Ogiya, O. Hahn, and A. Burkert, *Mon. Not. Roy. Astron. Soc.* **474**, 3043 (2018), [arXiv:1711.05276](https://arxiv.org/abs/1711.05276) [astro-ph.GA].
- [29] J. E. Taylor and A. Babul, *Astrophys. J.* **559**, 716 (2001), [arXiv:astro-ph/0012305](https://arxiv.org/abs/astro-ph/0012305).

- [30] F. C. van den Bosch, G. Tormen, and C. Giocoli, *Mon. Not. Roy. Astron. Soc.* **359**, 1029 (2005), [arXiv:astro-ph/0409201](#).
- [31] V. Berezhinsky, V. Dokuchaev, and Y. Eroshenko, *Phys. Rev. D* **77**, 083519 (2008), [arXiv:0712.3499 \[astro-ph\]](#).
- [32] J. Penarrubia and A. J. Benson, *Mon. Not. Roy. Astron. Soc.* **364**, 977 (2005), [arXiv:astro-ph/0412370](#).
- [33] R. Takahashi, *Wave Effects in the Gravitational Lensing of Gravitational Waves from Chirping Binaries*, Ph.D. thesis, Department of Physics, Kyoto University (2004).
- [34] W. H. Press and P. Schechter, *Astrophys. J.* **187**, 425 (1974).
- [35] J. R. Bond, S. Cole, G. Efstathiou, and N. Kaiser, *Astrophys. J.* **379**, 440 (1991).
- [36] D. J. Eisenstein and W. Hu, *Astrophys. J.* **496**, 605 (1998), [arXiv:astro-ph/9709112](#).
- [37] E. Retana-Montenegro, E. Van Hese, G. Gentile, M. Baes, and F. Frutos-Alfaro, *Astron. Astrophys.* **540**, A70 (2012), [arXiv:1202.5242 \[astro-ph.CO\]](#).
- [38] P. Jaranowski and A. Krolak, *Living Rev. Rel.* **8**, 3 (2005), [arXiv:0711.1115 \[gr-qc\]](#).
- [39] P. Amaro-Seoane *et al.*, *arXiv e-prints*, [arXiv:1702.00786 \(2017\)](#), [arXiv:1702.00786 \[astro-ph.IM\]](#).
- [40] T. Robson, N. J. Cornish, and C. Liu, *Class. Quant. Grav.* **36**, 105011 (2019), [arXiv:1803.01944 \[astro-ph.HE\]](#).
- [41] M. Lewicki and V. Vaskonen, *Eur. Phys. J. C* **83**, 168 (2023), [arXiv:2111.05847 \[astro-ph.CO\]](#).
- [42] E. Poisson and C. M. Will, *Phys. Rev. D* **52**, 848 (1995), [arXiv:gr-qc/9502040](#).